

Thermal baffling of SPHERE IFS

Raffaele G. Gratton^{a 1}, Riccardo U. Claudi^a, Enrico Giro^a, Umberto Anselmi^a, Dino Mesa^a, Luigi Lessio^a, Vincenzo De Caprio^b, Enrico Mattaini^b, Salvo Incorvaia^b, Enrico Santambrogio^b, Salvo Scuderi^c, Jean Luc Beuzit^d, Kjetil Dohlen^e, Pascal Puget^d, Jean Louis Lizon^f, Reinhold J. Dorn^f, Markus Kasper^f

^aINAF - Osservatorio Astronomico di Padova (Italy);

^bINAF-IASF Milano (Italy);

^cINAF - Osservatorio Astrofisico di Catania (Italy);

^dLab. d'Astrophysique de l'Observatoire de Grenoble (France);

^eLab. d'Astrophysique de Marseille (France);

^fEuropean Southern Observatory (Germany)

ABSTRACT

IFS is one of the scientific channels of SPHERE, the new high contrast imager for the ESO VLT telescope. IFS is an integral field spectrograph for the near IR (up to 1.65 micron), using a Hawaii II detector. To simplify opto-mechanical design, IFS has no cold pupil. To reduce thermal background, a cold filter fabricated by JDSU has been placed about 30 mm in front of the detector. This filter allows reducing thermal background by more than a factor 10^4 . We describe the design and implementation of the baffling required for proper use of this system: this includes a combination of a cold and a warm baffles, and appropriate choices of the coatings of the surfaces. We present the laboratory results obtained, which show that this system has a thermal background below 10 e-/pixels in the SPHERE working conditions.

Keywords: Infrared Instrumentation, Optical design, Spectrographs

1. INTRODUCTION

IFS is one of the scientific channels of SPHERE, the new high contrast imager for the ESO VLT telescope^[1]. IFS is an integral field spectrograph for the near IR (from 0.95 to 1.65 μm)^[2]. It uses a Hawaii II detector, which is sensitive up to about 2.7 μm , so that thermal background is an issue. The specification we adopted is such that thermal background should not be the dominating source of noise for any scientific application: in practice, this may be quantified to a specification of a thermal background of less than 20 e-/pixel. In the following we describe how we designed IFS in order to achieve this specification (Section 2), a model of the thermal background we used in the optimization process (Section 3), and the measurement made on the real instrument to verify that the adopted concept verifies the specification (Section 4).

2. CONCEPT

In order to simplify the opto-mechanical design, IFS is not a fully cryogenic instruments; specifically, no cold pupil was foreseen. The dewar window is flat, and there is no powered optical surface within the dewar. Rather, a low pass band filter (hereinafter LPB) fabricated by JDSU has been placed about 30 mm in front of the detector to achieve the specification on the thermal background². Temperature of this filter is kept very low (~ 150 K) so that its thermal emission is negligible. LPB allows reducing unwanted radiation over the wavelength range 1.7-2.7 μm by more than a factor 10^4 (see Figure 1). Since this is an interferential filter, it works properly only for rays incident with an angle close to normal, in practice approximately < 18 degree (see again Figure 1). The filter is used on the converging beam provided by the IFS camera: this is not an issue because the beam is very long (approximately $f/34$). However, to avoid leakage at long wavelengths, the cold filter should not see warm surfaces with large incidence angles, even if reflected by a single

¹ raffaele.gratton@oapd.inaf.it; phone ++39 0498293442; fax ++39 0498759840

² LPB filter also defines the longer wavelength of the spectra obtained with IFS.

surface with inorganic anodization, with reflectivity ~ 0.02 . This was achieved by combining a number of design features:

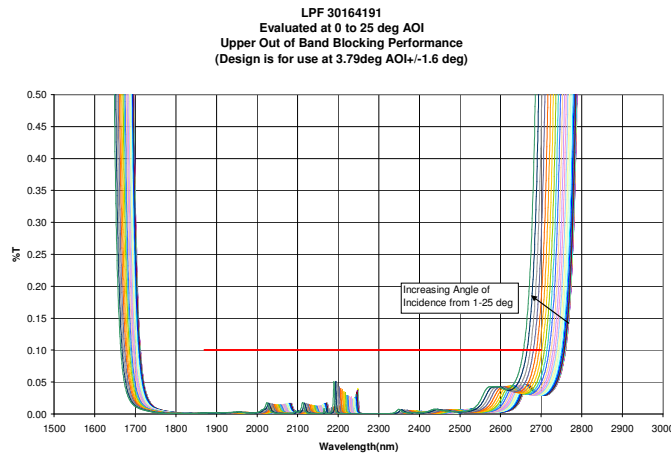


Figure 1 Transmission of the cold filter (LPB filter) in the range from 1500 to 3000 nm for different incidence angles (data from JDSU).

1. The dewar window (diameter of 48 mm) was located far from the LPB filter surface. This allows avoiding direct light from outside the dewar to impinge on LPB filter at angles larger than ~ 11 degrees; in this condition the LPB filter may then work properly. A distance of 105 mm is enough to guarantee specification. The optical design of the IFS camera was then optimized with the condition that the last powered surface is farther from the detector than 140 mm, and the dewar was designed in order to have such a long separation between the window and the detector (see Figure 2). The last powered surface of the camera is actually farther than this minimum value: this allows easy mounting and focusing of the IFS by moving the camera, which is at room temperature.
2. A cold baffle ($T \sim 150$ K) was located inside the dewar screening the warm inner surface of the dewar (see Figure 3). The front opening of this cold baffle is very close to the dewar window and its diameter is such that only the window is seen by the filter. Its external surface is bare aluminum to reduce the thermal coupling with the dewar wall; the inner surface is treated with inorganic black anodization (3M Black Velvet, reflectivity of $< 0.03^{[3]}$) to reduce the impact of reflections on the baffle itself. This is further reduced by an appropriate geometry of the baffle, which is a cylinder with three screens perpendicular to the optical path (each one with the minimum inner aperture allowed by the footprint of the beam at the corresponding locations). This design drastically reduces the possibility that light entering the buffer may impinge on the cold filter after single or even double reflection on it. In practice, only light reflecting three times on the interior of the cold baffle may reach the cold filter. This baffle is extremely effective in reducing the thermal background: when it is inserted within the instrument, thermal background is $\sim 10^4$ times smaller than what is obtained by removing it.
3. Thermal background was reduced by a further factor of ~ 4 by inserting a warm baffle around the last lens of the IFS camera. This is a spherical mirror, concentric to the center of the cold filter. The scope of the cold baffle is to ensure that the cold filter essentially looks itself that is a cold surface. Emissivity of this mirror is kept low by using an Al coating; in the future, we plan to replace this with a Au coated mirror. The mirror has an inner aperture of 34 mm, to allow light from the IFS to reach the detector; the outer diameter is kept as small as possible, compatible with the requirement that highly emitting warm surface is seen by the cold filter.



Figure 2. Photo of the dewar. Note the large distance between the window and the detector, which is roughly at the location of the widest flange.

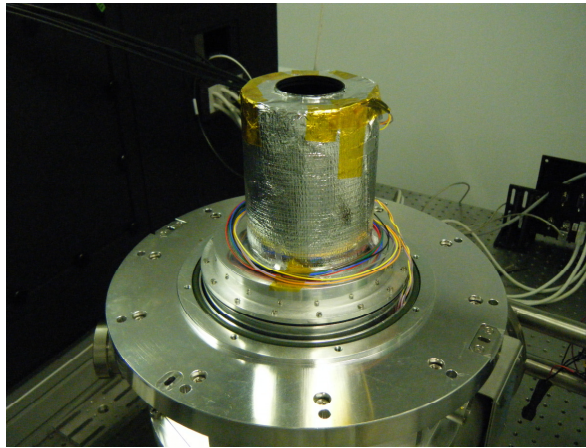


Figure 3. External view of the cold baffle mounted on the detector assembly.

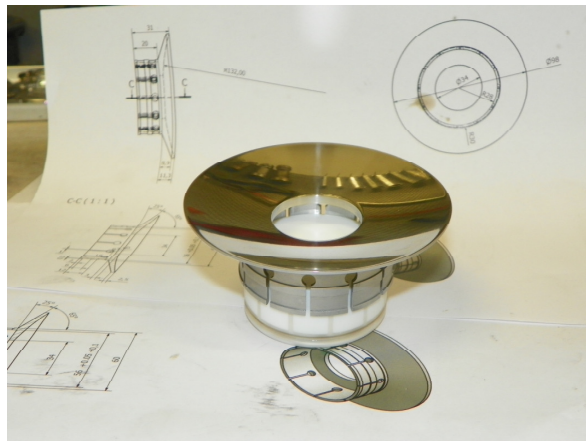


Figure 4. Photo of the warm baffle before being mounted on the IFS camera holder.

3. THERMAL BACKGROUND MODEL

A model was used to predict the thermal background flux incident on the detector. This value is actually estimated at field center, assuming this is valid throughout the whole detector.

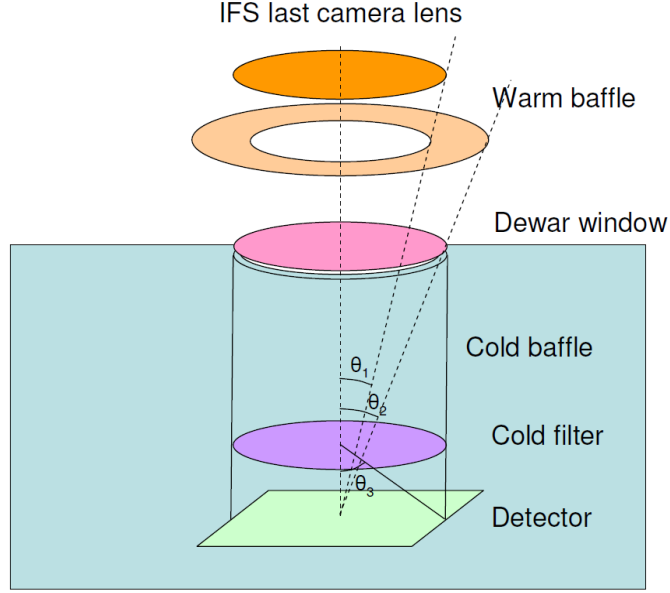


Figure 5. Schematic of IFS baffling

To understand how the model works, we may refer to Figure 5, which shows the IFS thermal baffling in a schematic way. Essentially, the IFS can be divided into two regions: the cold one (the light blue area of Figure 5), which is at a temperature T_D ($T_D \sim 140-150$ K), and the warm part outside the dewar (including its wall), which is at the environment temperature T_A ($T_A = 270-300$ K). As mentioned above, let us consider the center of the detector and assume that the IFS has a cylindrical symmetry around an axis passing through this point and normal to the detector surface. As seen from the detector, the solid angle within an angle θ_2 (≈ 0.197 radians) from this axis is seen at warm temperature, while that outside this area is seen at cold temperature. We will further assume that the emissivity η_1 of the area within θ_1 (≈ 0.081 radians); this is the last lens of the camera, through which the rest of the IFS is seen) is high (~ 1), while that of the area between θ_1 and θ_2 is kept small ($\eta_2 = 0.09$) by a reflecting Al coating of the surface of the warm baffle (that is spherical, roughly concentric to the cold filter, to avoid reflection of emission from the ambient to penetrate into the dewar). We have then three emission terms, corresponding to the cold baffle, the warm baffle and the last camera lens. Part of the light emitted from these surfaces will be stopped by the cold filter, whose transmission depends on the incidence angle θ and on wavelength λ .

In addition, the detector may see also light reflected from the cold baffle, which has a very low internal reflectivity $\rho = 0.025$ for the wavelength of interest ($0.95-2.7 \mu\text{m}$) by use of an appropriate surface treatment (inorganic anodization). The design of the cold baffle ensures that only a very small fraction of the surfaces may be seen by the detector in single reflection (the most important being the edge of the cold filter holder, that we will assume to reflect as a Lambertian surface), and that virtually no light can reach the detector after two reflections. However, triple reflections cannot be controlled. We then assume that the whole surface of the cold baffle can be seen by triple reflection of light entering its upper aperture, and that this source of light is distributed isotropically. Part of this light passes through the cold filter, mainly at large angles (the component at small angles being absorbed by the filter). To reduce this leakage, the wall of the chamber between the filter and the detector is inorganic anodized, so that almost all the light passing through the cold filter at angles $> \theta_3$ (≈ 1.06 radians) is absorbed onto these walls, and do not reach the detector itself.

In practice, the thermal background E is then the sum of five terms:

1) The emission from the last lens of the camera and beyond. This is:

$$E_1 = 2\pi \Delta\sigma \eta_1 \iint f(T_A, \lambda) g(\lambda, \theta) s(\lambda) \theta \cos \theta d\theta d\lambda, \quad (1)$$

where $\Delta\sigma$ is the pixel area ($324 \mu\text{m}^2$), $f(T_A, \lambda)$ is the Planck black body emission (expressed in number of photons) at a wavelength λ from a unit surface at temperature T_A , $s(\lambda)$ is the detection efficiency, the integral over the angle is from 0 to θ_1 , while that on λ is from 0 to infinity.

2) The emission from the warm baffle:

$$E_2 = 2\pi \Delta\sigma \eta_2 \iint f(T_A, \lambda) g(\lambda, \theta) s(\lambda) \theta \cos \theta d\theta d\lambda, \quad (2)$$

where the integral over the angle is from θ_1 to θ_2 , and that on λ is from 0 to infinity.

3) The emission from the cold baffle:

$$E_3 = 2\pi \Delta\sigma \eta_D \iint f(T_D, \lambda) g(\lambda, \theta) s(\lambda) \theta \cos \theta d\theta d\lambda, \quad (3)$$

where $\eta_D \sim 1$, the integral over the angle is from θ_2 to $\pi/2$, and that on λ is from 0 to infinity. This term is however negligible, given the low value of T_D .

4) The term due to reflection on the cold filter holder (this is the largest single reflection term).

This is assumed to be a Lambertian surface, reflecting a fraction ρ of the incident light, and is equal to:

$$E_4 = (2\pi)^2 \Delta\sigma (d_{CB}/d_{CF})^2 \eta_{CB} \rho \iint f(T_A, \lambda) g(\lambda, \theta) s(\lambda) \sin^2 \varphi (\pi/2 - \varphi) \theta \cos \theta d\theta d\lambda, \quad (4)$$

where:

$$\varphi = \pi/2 - \arctan[(2 l_{CB}/d_{CF}) - \tan \theta]. \quad (5)$$

l_{CB} being the length of the cold baffle, and d_{CF} the diameter of the aperture of the cold filter. In our case, we have $l_{CB} = 108$ mm and $d_{CF} = 48$ mm. The integration limits for the integration in θ may be set at $0.6 < \theta < 0.8$, and that on λ is from 0 to infinity.

5) The term due to multiple reflections:

$$E_5 = 2\pi \Delta\sigma (d_{CB}/d_{CF})^2 \eta_{CB} \rho^3 \iint f(T_A, \lambda) g(\lambda, \theta) s(\lambda) \theta \cos \theta d\theta d\lambda, \quad (6)$$

where d_{CB} and d_{CF} are the diameters of the aperture of the cold baffle and of the cold filter ($d_{CB} = 42$ mm), η_{CB} is the emissivity of the cold baffle aperture ($\eta_{CB} = 1$), the integral over the angle is extended from 0 to θ_3 (we neglect light reflected from the wall of the area between the filter and detector), and that on λ is from 0 to infinity.

Evaluating these terms, we assumed that the cold filter transmission $g(\lambda, \theta)$ can be written as $g(\lambda, \theta) = g(\lambda')$, where

$$\lambda' = [0.906308/\cos(\theta)]^{0.389} \lambda, \quad (7)$$

g being the filter transmission measured at 25 degrees incidence. This equation represents very well the transmission of this filter measured at various angles (see Figure 1).

Finally, the detector efficiency $s(\lambda)$ was assumed to be:

$$s(\lambda) = 0.90 \exp[-(\lambda/2.54)^{60}], \quad (8)$$

where λ is in micron.

Using these equations, we obtained e.g. the following contributions to thermal background for an ambient temperature of $T_A = 24^\circ\text{C} = 297.5$ K, and a cold baffle temperature of $T_D = 148$ K: Emission from last camera lens and beyond (IFS): $E_1 = 9.1$ photons/s/pixel; Warm baffle: $E_2 = 3.7$ photons/s/pixel; Cold baffle: $E_3 = 0.0$ photons/s/pixel; Single reflections on cold filter holder: $E_4 = 0.3$ photons/s/pixel; Triple reflections: $E_5 = 1.1$ photons/s/pixel.

4. EXPERIMENTAL RESULTS

The test simply consists in the acquisition of images with the IFS detector, with the IFS sealed. These were repeated at various temperature of the IFS bench. Results are listed in Table 1. Figure 6 shows the run of the median background with the bench temperature.

In this figure, we plotted the measured values (blue symbols), as well as three curves which represent:

- The run expected if the thermal background were due to short wavelength photons only (yellow line). This is close to expectations by our model.
- The run expected if the thermal background due to long wavelength photons only (cyan line).
- The run expected if only photons emitted by the active surface of the last camera lens are considered (with an emissivity equal to 1). This last curve represents the absolute minimum thermal background that might be obtained by a perfect thermal design of the IFS.

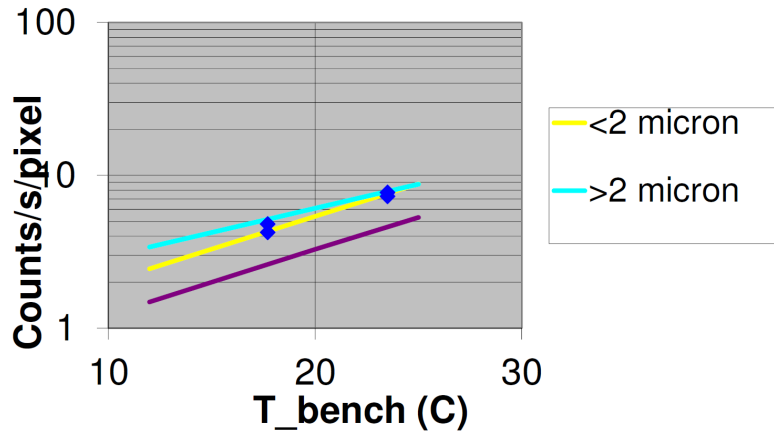


Figure 6. Run of IFS background as a function of temperature (blue symbols). Overimposed are the expected run when background is dominated by photons with wavelength $< 2 \mu\text{m}$ (yellow curve; this curve is indistinguishable from the predictions of our model) or long wavelength ones ($> 2 \mu\text{m}$: cyan curve). Violet line represents expectations when only photons emitted from the last camera lens are considered.

Table 1. Median background measured at various bench temperatures

Date	Prism	Exposure	Bench Temp.	Measures		Model			
				Median	Median	IFS	Warm Baffle	Multiple refl.	Total
		s	C	counts/s/pixel		e ⁻ /s/pixel			
31/03/2011	Open	50x10	17.7	4.24	7.6	4.9	2.0	0.7	7.6
31/03/2011	Open	1x3600	17.7	4.81	8.7				
4/04/2011	Open	50x10	23.5	7.29	13.1	8.7	3.5	1.4	13.7
4/04/2011	Open	1x3600	23.5	7.74	13.9				
19/04/2011	Open	1x3600	24.0	7.83	14.1	9.1	3.7	1.5	14.3

Measured data are about 1.5 times the theoretical absolute minimum. This is explained by our model (see the last four columns of Table 1, where results for the main individual components are given). According to our model, the most significant source of background is thermal emission seen through the IFS camera, which cannot be eliminated. This is followed by the warm filter, which is expected to contribute almost a fourth of the total. A minor contribution (about 10% of the total) comes from multiple reflections within the cold baffle. Thermal background is very good. Using our model, which fits very well data and is virtually indistinguishable from the yellow curve of Figure 6, we can extrapolate the value at 12 C, which is the maximum operational temperature: we get a value of 2.5 counts/s/pixel, corresponding to 4.5 e⁻/s/pixel (the conversion factor is 1.8 e⁻/counts), well within specification.

REFERENCES

- [1] Beuzit, J.-L., Feldt, M., Dohlen, K., et al., "SPHERE: a planet finder instrument for the VLT", Proc. SPIE, 7014, 701418-701418-12 (2008)
- [2] Claudi, R.U., Turatto, M., Giro, E., et al. "SPHERE IFS: the spectro differential imager of the VLT for exoplanets search", Proc. SPIE, 7735, 77350V-77350V-11 (2010)
- [3] <http://www.freepatentsonline.com/4111762.pdf>